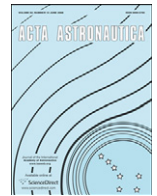




ELSEVIER

Contents lists available at SciVerse ScienceDirect

Acta Astronautica

journal homepage: www.elsevier.com/locate/actaastro

A personal airbag system for the Orion Crew Exploration Vehicle[☆]

Sydney Do^{a,*}, Olivier de Weck^{a,b}

^a Department of Aeronautics and Astronautics, Massachusetts Institute of Technology, Cambridge, MA, United States

^b Engineering Systems Division, Massachusetts Institute of Technology, Cambridge, MA, United States

ARTICLE INFO

Article history:

Received 28 February 2012

Received in revised form

13 June 2012

Accepted 24 June 2012

Keywords:

Orion

Landing

Airbag

Impact attenuation

Crew

ABSTRACT

Airbag-based methods for crew impact attenuation have been highlighted as a potential simple, lightweight means of enabling safe land-landings for the Orion Crew Exploration Vehicle, and the next generation of ballistic shaped spacecraft. To investigate the feasibility of this concept during a nominal 7.62 m/s Orion landing, a full-scale personal airbag system 24% lighter than the Orion baseline has been developed, and subjected to 38 drop tests on land. Through this effort, the system has demonstrated the ability to maintain the risk of injury to an occupant during a 7.85 m/s, 0° impact angle landing to within the NASA specified limit of 0.5%. In accomplishing this, the personal airbag system concept has been proven to be feasible. Moreover, the obtained test results suggest that by implementing anti-bottoming airbags to prevent direct contact between the system and the landing surface, the system performance during landings with 0° impact angles can be further improved, by at least a factor of two. Additionally, a series of drop tests from the nominal Orion impact angle of 30° indicated that severe injury risk levels would be sustained beyond impact velocities of 5 m/s. This is a result of the differential stroking of the airbags within the system causing a shearing effect between the occupant seat structure and the spacecraft floor, removing significant stroke from the airbags.

© 2012 Elsevier Ltd. All rights reserved.

1. Introduction

Since the start of its development in late 2006, the Orion Crew Exploration Vehicle (CEV—now named the Orion Multi-Purpose Crew Vehicle, or MPCV) has experienced several modifications to its landing system architecture. One aspect which has been regularly revisited throughout the program is the baseline mode in which the vehicle is to land on the Earth's surface, and consequently the concept which should be employed to facilitate this landing. This uncertainty has been linked to a combination of a strained mass budget, and difficulties in developing systems capable of protecting astronauts

during all possible landing scenarios [1]. This paper presents the work that was conducted to evaluate the feasibility of implementing an alternative, lightweight, airbag-based crew impact attenuation system within the cabin of the Orion Crew Module, in order to facilitate safe land-landings. This was achieved through the complete design, development, and drop testing of a full-scale personal airbag system.

2. Background and motivation

It is a remarkable fact that every capsule-shaped reentry vehicle developed by NASA initially had a specific requirement to land on land, but was ultimately designed to land in water, due to the technical and schedule risks involved. With the schedule pressures of the Cold War space race long gone and the desire to develop a sustainable, long-term space transportation program, there was

[☆] This paper was presented during the 62nd IAC in Cape Town.

* Corresponding author. Tel.: +1 8572048716.

E-mail addresses: sydneydo@mit.edu (S. Do), deweck@mit.edu (O. de Weck).

an interest at the program’s inception in developing a land-landing capability for Orion.

Inherently more challenging than the traditional “splashdown” mode, the desire for land-landing arises primarily from considerations related to the recovery and refurbishment of the vehicle. Recovery from the sea introduces challenges in keeping the target vehicle afloat, and in gaining access to the vehicle as it rests in the dynamic marine environment [2]. Contrastingly, land-landings facilitate easier egress and vehicle recovery, while also mitigating the risk of water damage. This latter attribute has implications on the ease of refurbishment and reusability of the spacecraft, which in turn impacts the life-cycle costs of the program [1]. The disadvantage of employing a land-landing mode, however, is that higher accelerations are imparted upon the crew during impact. This hence requires a more complex, and inevitably higher mass impact attenuation system.

During a preliminary study conducted by the NASA Engineering and Safety Center (NESC) in early 2007, the risks and costs involved in land versus water landings for Orion were assessed [2]. From this, it was concluded that the operational and life-cycle benefits of nominal land-landings far offset their inherent additional complexity, resulting in a recommendation for Orion to adopt a primary land-landing mode. To support this development, the NESC further recommended that injury-risk mitigation options be

investigated for land-landings. Here, a specific mention was made to:

“Pursue an alternate approach to the internal astronaut couch attenuation system based on difficult experience with (the) Apollo strut support system. The current CEV design of the astronaut couch and associated couch attenuation system should be revisited” (Fig. 1) (Ref. [2]).

To address this, a workshop was conducted by the NESC in the summer of 2008 [3], where a team of academic and industry experts were tasked to develop alternative concepts to the Apollo-era couch-based design. Moreover, prior to this workshop, a decision was made for Orion to revert back to a nominal water-landing mode in an attempt to bring the vehicle back to within its mass allocation, thus motivating the need for the developed concepts to be lightweight. As a result, the idea of the personal airbag system was born.

Inspired from the structure of endospermic seeds in nature, this concept involves using an inflated airbag “seat” to protect the occupant during landings of the Orion crew module. Just as these seeds protect their embryos from mechanical loads by surrounding them with a layer of endosperm, this concept involves surrounding the astronaut in a personal cushion of air. When crew positioning requirements were factored, this concept evolved into the personal airbag system. The original ideation process used to develop this concept is shown below in Fig. 2.

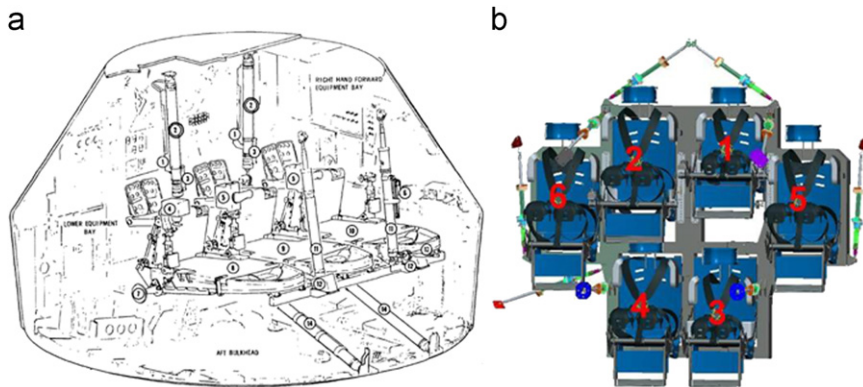


Fig. 1. Comparison of Apollo and baseline Orion crew impact attenuation systems. Both systems are based on the same concept of a rigid pallet carrying crew seats, supported by shock absorbing struts (a). Apollo [4] (b). Current Orion baseline [1].

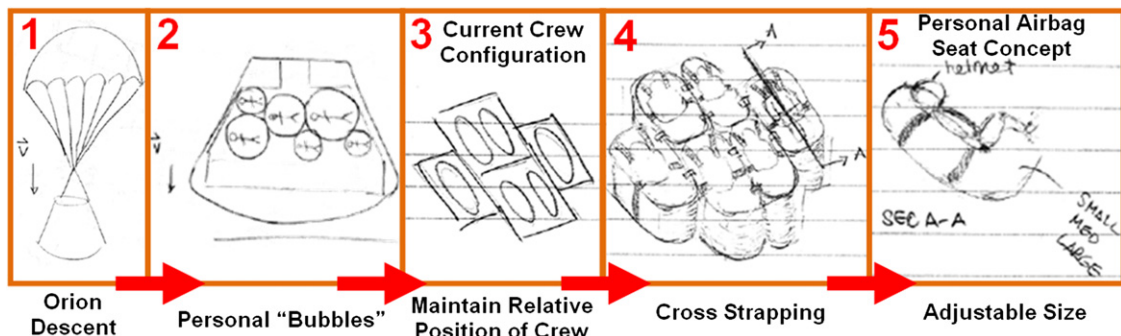


Fig. 2. Original ideation process used to conceptualize the personal airbag system.

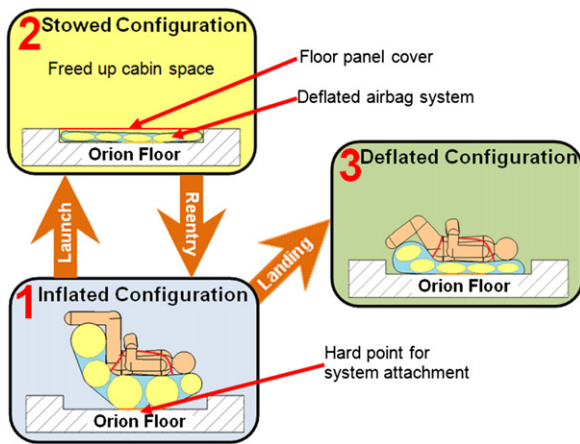


Fig. 3. System concept of operations consisting of the inflated, stowed, and deflated configurations. During pre-launch and launch, the system would be in the inflated state to function as a seat to support the occupant. Once in space, the system would transition to the stowed state to increase available cabin volume. Prior to reentry, the system is then returned to its inflated state in preparation for landing. Upon landing, the seat transitions to the deflated state as it attenuates the impact loads subjected to the crew.

In addition to being inherently lightweight, this system has the advantage of being able to be deflated and stowed when not in use, thus providing additional in-cabin volume. Initial estimates found that a potential 36% reduction in the mass without the crew, and an increase in 26% of in-orbit habitable volume [5] could be obtained, as compared to the baseline Orion system. From an operational viewpoint, this latter attribute is beneficial both when the spacecraft is in orbit, and seats are no longer required; and after landing, where the deflated system enables easier egress of the vehicle as compared to the baseline design. This becomes particularly important in contingency situations where a quick egress from the vehicle is desired. Fig. 3 depicts the system concept of operations.

3. Development approach

To investigate the impact attenuation potential of the personal airbag system concept, a three-level spiral model of system development was employed [7]. This involved cycling through the complete development process, from system conception through to its detailed design, implementation, and operation, three times. In each subsequent cycle, lessons learned from the previous were used to develop an improved next generation of the system. (Fig. 4.)

Specifically, the first spiral focused on developing and testing a complete analog airbag system (Fig. 5a). Through this effort, insights into the relative positioning of the airbags with respect to the occupant support structure, as well as the system failure modes were obtained. The development and testing of this system, as well as the lessons learned from this effort are extensively described in Ref. [6].

From these lessons learned, a single airbag drop test article was built in the second spiral to investigate the

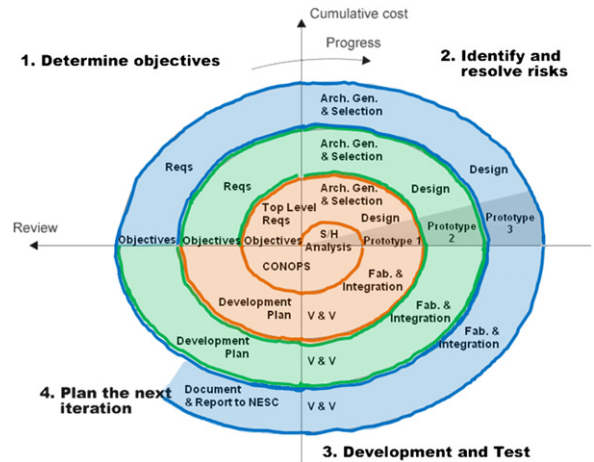


Fig. 4. Three level spiral model (Adapted from Ref. [7]).

impact dynamics of a single airbag (Fig. 5b). The obtained test results were then used to validate previously formulated impact models (see Section 4.2.). In addition, this second spiral led to the in-house development, testing, and validation of flapper valves, as well as the determination of airbag manufacturing techniques, including airbag stitch patterns, and treatment methods for fabric leakproofing (see Ref. [8]).

Using the experience and data gained from the first two development spirals, a full-scale personal airbag system was then developed and subjected to a series of drop tests in the final spiral, thus allowing for the feasibility of the concept to be determined.

4. System modeling

As was conducted throughout all development spirals, the development of the full-scale personal airbag system consisted of firstly developing a baseline airbag configuration based upon knowledge obtained from previous design spirals; followed by optimizing the size of the individual airbags such that the injury risk subjected to the occupant was minimized. The following sections describe the airbag impact and injury-risk models that were developed to accomplish this.

4.1. The Brinkley direct response index

To ensure a common framework for measuring injury-risk to astronauts during transient acceleration environments, NASA has mandated that the Brinkley direct response index (DRI) be used in the design and development of all human spacecraft crew impact attenuation systems [9]. This index measures the risk of injury to an occupant given a measured acceleration profile by comparing the output of a dynamics model of the human body, to limiting values representing varying levels injury-risk (Table 1). In order for a system to be considered safe, the maximum Brinkley DRI experienced during an acceleration event must remain within the “low” injury-risk bounds, which equates to a 0.5% likelihood of injury sustained anywhere on the body.

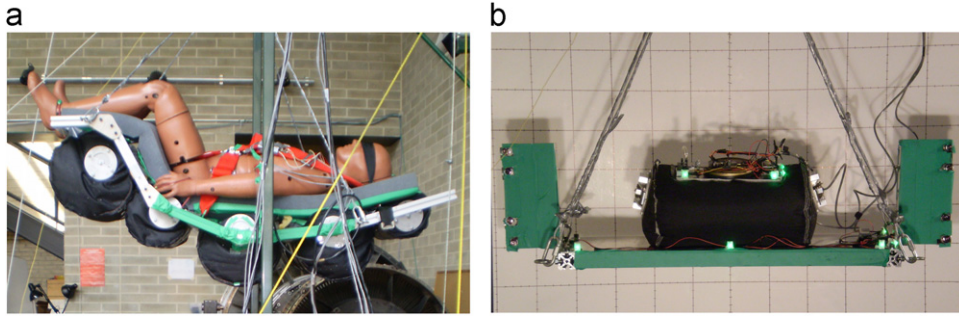


Fig. 5. (a) Analog airbag system. (b) Single airbag drop test article.

Table 1

NASA HSIR specified Brinkley DRI limits (Refs. [9,10]).

Brinkley DRI limit level	x		y		z	
	DRI _x < 0	DRI _x > 0	DRI _y < 0	DRI _y > 0	DRI _z < 0	DRI _z > 0
Very low (0.05%)	−22.4	31	−11.8	11.8	−11	13.1
Low (0.5%—safe limit)	−28	35	−14	14	−13.4	15.2
Moderate (5%)	−35	40	−20	17	−12	18
High (50%)	−46	46	−30	22	−15	22.8

Note that the percentage values listed next to the Brinkley DRI limit levels correspond to the likelihood of injury to the occupant at any location on the human body.

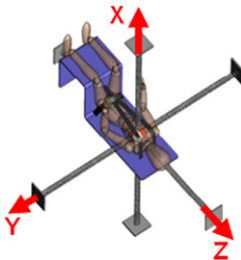


Fig. 6. Brinkley direct response index model [10].

Here, the response of the human body is treated as that of a spring-mass-damper system in each of the three orthogonal axes, referenced to the center of the torso (Fig. 6). A simplifying assumption made, is that the effects of the applied acceleration profile in each of the three axes are decoupled. This dynamic system is modeled with the relationship given in Eq. (1).

$$\ddot{X}(t) + 2\zeta\omega_n\dot{X}(t) + \omega_n^2X(t) = A(t) \quad (1)$$

where X is the relative displacement coordinate of the dynamic system relative to the center of the torso in the x -, y -, or z -direction. Here, a positive value corresponds to a compression; A is the measured acceleration profile from the reference point in the x -, y -, or z -direction; ζ is the damping ratio of the dynamic system in the given x -, y -, or z -direction (Table 2); ω_n is the natural frequency of the dynamic system in the given x -, y -, or z -direction (Table 2); and t is a time coordinate.

Table 2

NASA HSIR specified natural frequencies and damping ratios to be used in the Brinkley dynamic response model (Ref. [9]).

	x	y	z
ω_n (rad/s)	62.8	58.0	52.9
ζ	0.2	0.09	0.224

The Brinkley DRI is obtained by solving the system given by Eq. (1) and inputting the result into the following relationship:

$$DRI(t) = \frac{\omega_n^2 X(t)}{g} \quad (2)$$

where g is the acceleration due to the Earth's gravity, used here as a normalizing factor.

4.2. Single airbag impact model

Fundamentally, airbags attenuate impact loads by converting the kinetic energy of an impacting object into the potential energy of the airbag gas, as the object does boundary work on the airbag. This energy is then removed from the system by venting the gas. Depending on the amount of gas vented, the system will either experience a bounce after the initial impact or come to an immediate rest. In this regard, airbags can be considered as non-linear springs, whose stiffness is dependent on the airbag geometry and venting characteristics. This is particularly apparent when performing a force equilibrium in the vertical

direction on the idealized airbag system, as depicted in Fig. 7. This yields the following equation:

$$\underbrace{m\ddot{x}}_{\text{Acceleration}} + \underbrace{(P_{bag}(x) - P_{atm})A_{FP}(x)}_{\text{ReactionForce}} = \underbrace{mg}_{\text{Weight}} \quad (3)$$

Where m is the payload mass, P_{bag} is the airbag pressure, P_{atm} is the atmospheric pressure, and A_{FP} is the airbag footprint area. Moreover, it can be seen that this equation is in the form of a mass-spring system, with a nonlinear spring stiffness, given by

$$k(x) = \frac{1}{x(t)}(P_{bag}(x,t) - P_{atm})A_{FP}(x) \quad (4)$$

From this form, it can be seen that this nonlinear stiffness is the result of the interaction between the airbag pressure and its geometry. When the combination of these variables is appropriately chosen, it is this nonlinearity which yields the damping effectively experienced by the payload mass during impact. In order to determine the values of these variables, a framework based on the original dynamics model used to develop the Mars Pathfinder airbag system [11] was implemented. Specifically, this framework treats the airbag impact attenuation problem from a fluid mechanics perspective, using an Euler time stepping scheme to determine the change in airbag geometry based on the vertical position of the supported mass at each time increment. This geometry solution is then used to obtain the pressure, volume, and mass of the operating medium, which is in turn used to determine conditions for the venting of the airbag. Fig. 8 presents a top level N² diagram of the model.

In order to obtain the injury-risk response of the supported payload during a given impact event, the acceleration response obtained from executing the single

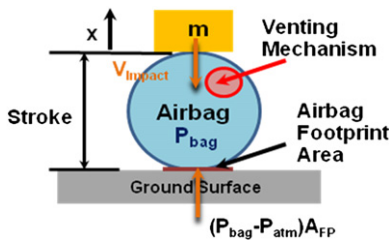


Fig. 7. Idealized single airbag impact case.

airbag model is input as the forcing function into Eq. (1). From this, the Brinkley DRI is obtained and compared to the limits given in Table 2, thus yielding the injury-risk subjected to the occupant. The full derivation of all equations used to develop this model is provided in Refs. [8] and [11].

Furthermore, this model was validated during the second development spiral discussed in Section 3, by using the results obtained in the single airbag drop test campaign. Specifically, drop tests were performed at varying drop heights to characterize the system dynamics at different impact velocities. A comparison of the predicted and experimentally measured impact acceleration profiles is presented in Fig. 9.

4.3. Design space exploration

In addition to validating the single airbag impact model, a study was performed to gain insight into the effects of the airbag design variables on the overall system performance. This involved using the model to perform a full factorial expansion of the design space for a single airbag with a fixed payload mass (Fig. 10), and performing a sensitivity analysis on the resulting objective space from the standpoint of simultaneously minimizing the peak Brinkley DRI and the overall system mass. This yielded two key findings:

- For a fixed airbag geometry, the Brinkley response is most sensitive to changes in the venting area. This can be explained by considering the energy exchanges that occur during the impact process. Fundamentally, the venting area dictates the amount and rate at which gas is vented from the airbag, which in turn, equates to the amount of energy being removed from the system
- For a system using pressure relief valves, the mass and injury-risk optimal design is one with the minimum airbag geometry such that bottoming-out (i.e. direct contact between the payload mass and the impacting surface) does not occur.

This finding arises from the unintuitive observation that systems with lower peak Brinkley DRI values tended to have

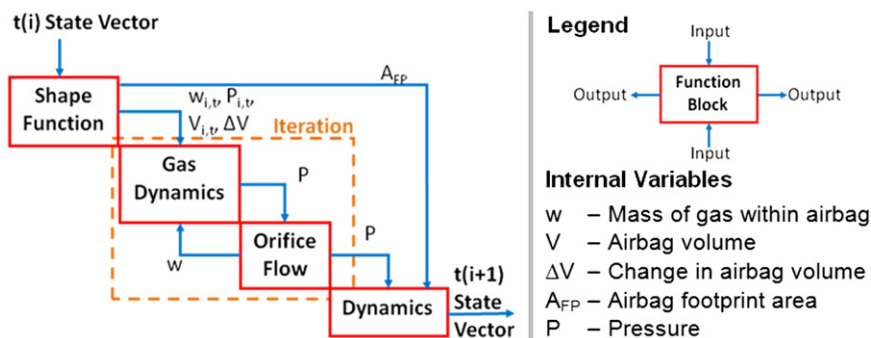


Fig. 8. Single airbag impact model top level N² diagram.

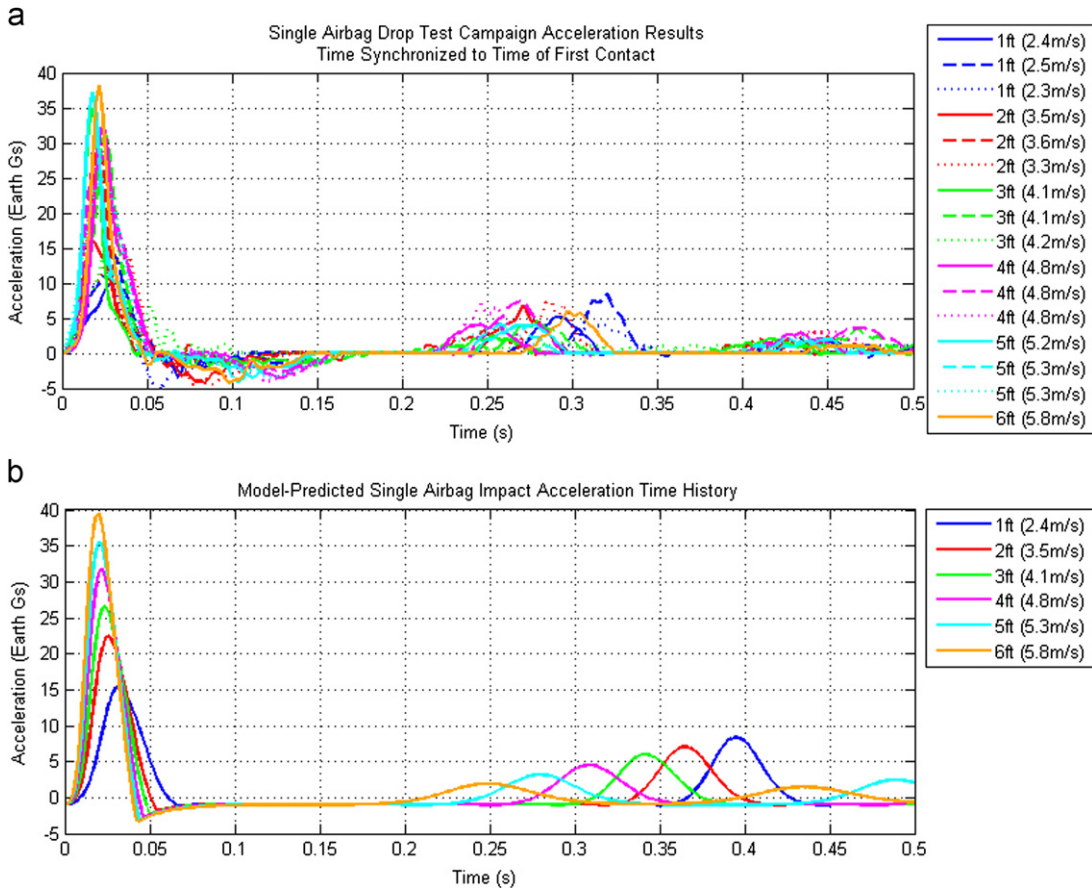


Fig. 9. Comparison between experimentally-obtained, and model-predicted acceleration profiles. (a) Experimentally obtained data. (b) Model prediction. Legend reads: Drop height in feet (Impact velocity in m/s).

smaller geometries. This is because under the same impact conditions, smaller airbags are able to maintain a higher pressure over a longer period of time, causing the pressure relief valves to remain open for a longer period of time. This effectively increases the cumulative venting area when integrated over the impact duration, thereby allowing more gas to exit the system, and leading to improved impact attenuation. The lower bound on this geometry occurs when there is insufficient stroke to remove all kinetic energy from the payload mass prior to it directly impacting the landing surface.

4.4. Multi-airbag Modeling

With a validated single airbag impact model established, a multi-airbag impact model was developed to facilitate the design of the personal airbag system. This model exploits the non-linear stiffness of airbags by employing a structural dynamics framework, based on Lagrange's equation. This is given by

$$\frac{d}{dt} \left(\frac{\partial K}{\partial \dot{q}} \right) - \frac{\partial K}{\partial q} + \frac{\partial V}{\partial q} + \frac{\partial D}{\partial \dot{q}} = \frac{\partial W}{\partial q} \quad (5)$$

where K is the kinetic energy, V is the elastic potential energy, D is the damping on the system, W is the work done on the system, q is a generalized coordinate, and t is a measure of time.

Here, a two-degree of freedom model was employed, capturing the system vertical displacement and pitch angle. Combined, these degrees of freedom represent all the dynamics in the Brinkley x -direction—the direction in which the injury-risk criteria are most difficult to meet. Fig. 11 presents an idealized three airbag representation of the modeled system.

Using Lagrange's equation, the resulting system equations for this particular three airbag system are found to be

$$m\ddot{u} + k_1 u_1 + k_2 u_2 + k_3 u_3 = mg$$

$$J\ddot{\theta} - L \cos \theta (k_1 u_1 - k_3 u_3) = mg L_{Load} \cos \theta \quad (6)$$

where u is the system vertical displacement, θ is its pitch angle, u_i and k_i are respectively the vertical displacement and non-linear stiffnesses of airbag i , P is the system weight force located at its center of gravity, L is the distance between adjacent airbags, L_{Load} is the distance between the center of gravity and the system geometric center, m is the system mass, and J is its mass moment of inertia.

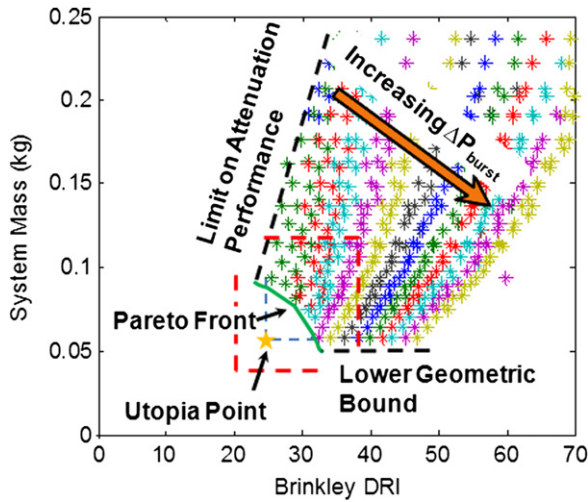


Fig. 10. Full factorial expansion of the objective space leading to the second key finding discussed above. Points of the same color relate to those with the same valve burst pressure. The utopia point refers to the notional design that simultaneously achieves both minimum system mass and minimum injury-risk. Because the physics of the problem prevents these two objectives from being simultaneously met, a “front” of “optimal” solutions occurs, called the Pareto front. These represent designs that best meet the spectrum of weighted combinations of the two objectives. Moving along the Pareto front shown in this figure corresponds to varying the valve burst pressure at the minimum airbag geometry such that bottoming-out does not occur.

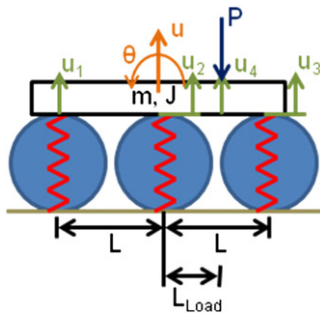


Fig. 11. Two degree of freedom multi-airbag model. Here, a three airbag configuration is shown.

To facilitate the design process, the multi-airbag model was structured such that the only inputs were the initial impact conditions and an airbag sizing and configuration combination. From this, the system equations were automatically derived using Eq. (6), and solved using a finite difference scheme to obtain the resulting Brinkley response. Note that the full derivation of the underlying equations used in this model can be found in Ref [8].

5. Personal airbag system configuration design and sizing

Using the multi-airbag model, the configuration of the personal airbag system was designed to maintain the Brinkley DRI to within low injury risk limits during land-landings at the Orion nominal impact velocity of

7.62 m/s (25 fps) (from Ref. [12]), and at impact angles of both 0° and 30° pitch forward. These impact angles were chosen based on an earlier NESC finding that flatter impact angles are preferable for land-landings [2], and that Orion is currently planned for a nominal 30° impact angle. Further constraints were also added to limit the design space, as summarized in the following problem formulation:

$$\text{Minimize } J(x) = [\max(\text{Brinkley DR}_x) \quad \max(\text{Brinkley DR}_z)]^T$$

where:

$$x = \text{Design Vector} = \begin{bmatrix} \text{Number of airbags}(N) \\ \text{Airbag radius}(R) \\ \text{Airbag length}(L) \\ \text{Valve burst pressure}(\Delta P_{burst}) \\ \text{Orifice area}(A) \end{bmatrix}$$

Subject to:

Airbag geometry=Cylindrical

Fixed airbag geometry: The cylinder was chosen as the baseline airbag geometry throughout this development effort for its ease of manufacturability.

$$2R(N - 1) \leq 1.5 \text{ m}$$

Geometric Constraint: Prevents geometric interference between airbags on the system. 1.5 m corresponds to the height of the crash test dummy used for testing when seated in the semi-supine position. See Ref. [8] for details regarding the choice of this position.

$$\begin{aligned} R_i &= R \\ L_i &= L \\ A_i &= A \\ P_{bag,i} &= 102 \text{ kPa} \end{aligned}$$

Commonality Constraints: Improves system robustness and eases manufacture.

Fixed Inflation Pressure:

Determined from experimental experience during the Second Development Spiral.

$$\sigma = \max(P_{bag}(X))R/t < 540 \text{ MPa}$$

(NB. *t* = Airbag material thickness)

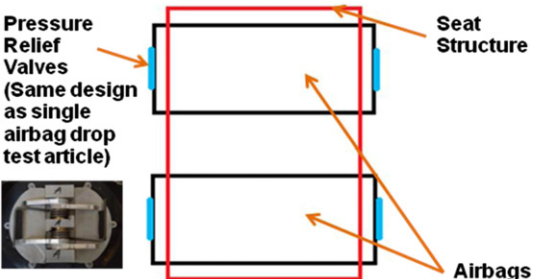
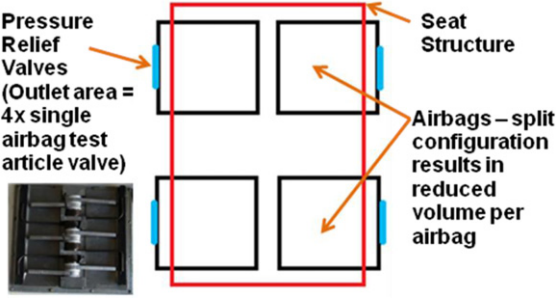
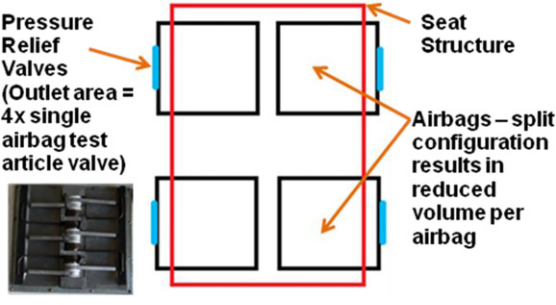
Hoop Stress Constraint: Ensures that the airbags do not rupture during impact. The upper bound was determined from material tensile strength tests performed during the Second Development Spiral.

From preliminary executions of the model, it was found that the system experienced a significantly higher injury-risk at impact angles of 30° as compared to those at 0°. Consequently, a 30° impact angle was baselined for this design effort as any system that performed adequately under this condition would easily meet the injury-risk requirements under a 0° impact condition.

With this, a two stage full factorial based methodology was employed to determine the “optimal” solution. This involved firstly performing a coarse resolution full factorial expansion to filter out hoop-stress-infeasible regions within the design space. When a feasible bounding region was found, a second, high resolution full factorial analysis was performed, allowing the set of minimum Brinkley DRI designs to be evaluated. From this, a decision to modify the configuration concept was made if all design solutions were found to be infeasible. In total, this process was iterated through three times, with each cycle exploring a unique airbag and valve configuration. The decisions

that were made throughout this process are summarized below

injury-risk criteria in the *x*-direction, as compared to the *z*-direction. This design is highlighted by the orange star

Configuration	Top view
<p>Iteration 1 Conventional configuration Based on the originally conceptualized personal airbag system. This configuration consists of a row of cylindrical airbags aligned in the longitudinal axis of the seat structure. Observations and conclusion Even when ignoring the hoop stress criterion, the best performing design was found to have an <i>x</i>-direction Brinkley DRI of 67.59 — a value which far exceeds the limiting value of 28. Thus, a drastic configuration change was required.</p>	
<p>Iteration 2 Split-bag 1-sided venting configuration Based on findings made in Section 4.3, the intent here was to halve the airbag volume and to quadruple the venting area of each airbag. Observations and conclusion All designs that met both hoop stress and injury-risk criteria were found to have large aspect ratios (largest airbag axial length of 0.2 m, with airbag radii of 0.32–0.34 m). These are highly susceptible to local buckling during impact, which has implications on system stability during impact.</p>	
<p>Iteration 3 Split-bag 2-sided venting configuration Here, the venting area on each airbag was doubled to further improve impact attenuation capability. This was based on the findings discussed in Section 4.3. Summary and Conclusions The maximum airbag length from the set of hoop stress and injury-risk feasible designs increased to 0.28 m (with the same airbag radii of 0.32–0.34 m). Lengths of this value were deemed appropriate for maintaining adequate impact stability. Thus, this configuration was baselined.</p>	

With the general system configuration baselined, the specific number of airbags in the longitudinal direction and the final geometry of the bags were finalized by introducing a seam stress limit of 90MPa to the design space. The intent of this was to prevent rupturing of the airbags during impact. Fig. 12 presents the resulting objective space.

It can be seen in Fig. 12 that the Brinkley performance moves very close to the low injury-risk limit when the airbag length is 0.28 m, as compared to a length of 0.26 m. It can be further observed that the additional system stiffness of the three-airbag configurations increases the *x*-direction Brinkley Index from the two-airbag case by a comparable amount. Moreover, the seam stress criterion was found to have made four of the originally non-dominated designs infeasible, thus limiting the final choice of the system configuration to the set of designs encircled by the orange ellipse. From this set, the design with the lowest *x*-direction Brinkley Index was chosen due to the substantially higher difficulty in meeting the

in Fig. 12, while its characteristics and predicted performance are respectively summarized in Table 3 and Fig. 13. Note that the final inflation pressure shown in Table 3 is close enough to atmospheric pressure such that a simple hand pump could be used to inflate the airbags. Although manually inflating the system may not be a desired nominal operation, the option of using this simple option introduces a robust contingency mode, which ultimately results in improved system safety.

6. Personal airbag system development and test plan

With a final design for the personal airbag system established, the development moved into a focused build and integration phase. This resulted in a system which weighed 24% less than the equivalent Orion crew impact attenuation system without any mass optimization purposefully implemented (see Table A1 in the Appendix for a detailed mass comparison of the two systems). With

this phase complete, a test plan consisting of two sessions was developed, corresponding to impact angles of 0° and 30°. During each session, drop tests were performed from heights of 1–10 ft in 1 ft increments. At each height, a minimum of two drop tests were performed to ensure repeatability of the obtained data.

With regard to data acquisition, a set of tri-axial accelerometers embedded in the chest of a crash test dummy was used to evaluate the Brinkley response, while two perpendicularly separated high speed cameras

were used to track LEDs installed about the system. This footage was post processed using photogrammetric analysis techniques to extract transient dynamics data (Fig. 14).

7. Test results and analysis

Throughout the month of August 2010, 38 drop tests were successfully performed with the personal airbag system. The first test session was successfully completed with a maximum impact velocity of 7.85 m/s achieved—a value higher than the nominal 7.62 m/s landing of the Orion CEV. The second test session however, concluded after a drop from 7 ft, when a tear was found at the lower hardpoint-to-fabric interface on one of the airbags (see Fig. 21). Closer inspection of the airbag and high speed camera footage indicated that this tear was a result of the formation of a local stress concentration. In particular, this was due to a shearing effect induced on the airbag as the seat structure slid forward relative to the simulated floor during the inclined impact. Although this failure led to the early conclusion of the drop test campaign, a sufficient data set had been obtained to determine system feasibility.

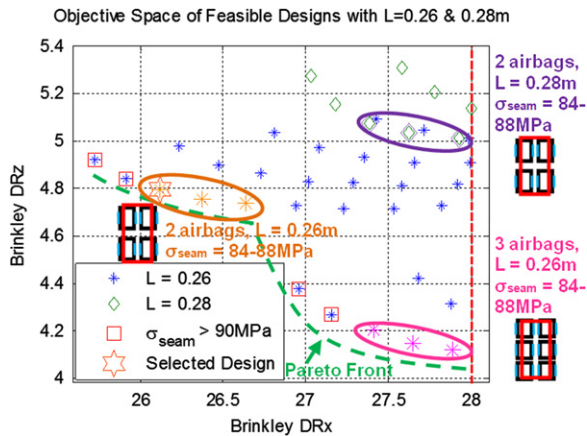


Fig. 12. Objective space filtered by Max Hoop stress < 540 MPa and L=0.26 m or 0.28 m. (For interpretation of the references to color in this figure legend, the reader is referred to the web version of this article.)

7.1. Test session 1 Results (0° impact Angle)

Fig. 15 shows the injury-risk results obtained from all Session 1 drop tests, while Table A2 in the Appendix provides a summary of this data.

Table 3
Final personal airbag system configuration.

Design variable	Value
Airbag configuration	Split bag 2-sided venting
Number of airbags	2
Valve type	Pressure relief valve with 4 × area of single airbag drop test article
Valve burst pressure	8 kPa
Airbag radius	0.32 m
Airbag length	0.26 m
Airbag inflation pressure	102 kPa
Predicted peak X-direction Brinkley	16.6 (0° Impact angle) 26.1 (30° Impact angle)
Predicted peak X-direction acceleration	11.8 Gs (0° Impact angle) 18.0 Gs (30° Impact angle)

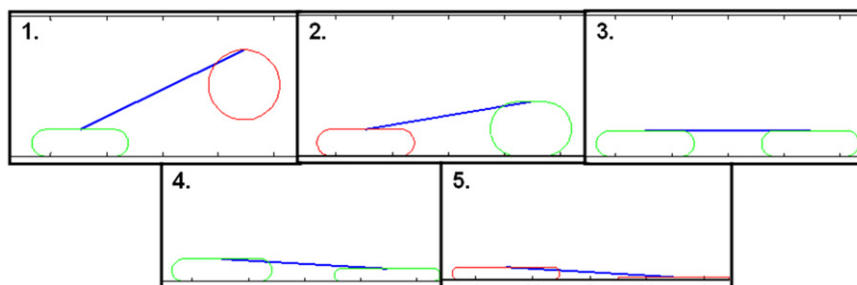


Fig. 13. Predicted system dynamic for the nominal 30° impact case (red= valve closed, green= valve open). (For interpretation of the references to color in this figure legend, the reader is referred to the web version of this article.)

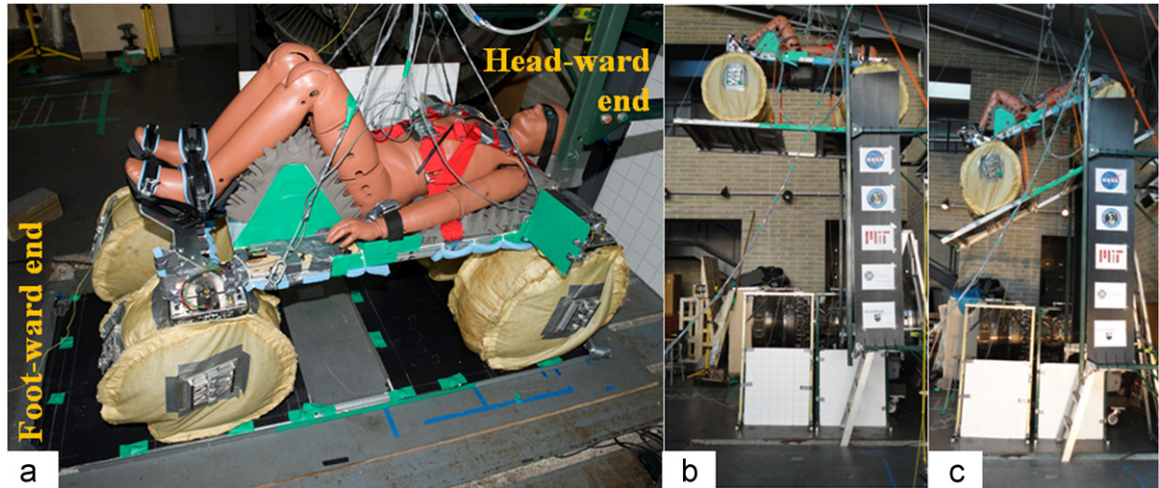


Fig. 14. (a) Fully integrated personal airbag system drop test configuration, (b) test session 1—0° impact angle and (c) test session 2—30° impact angle.

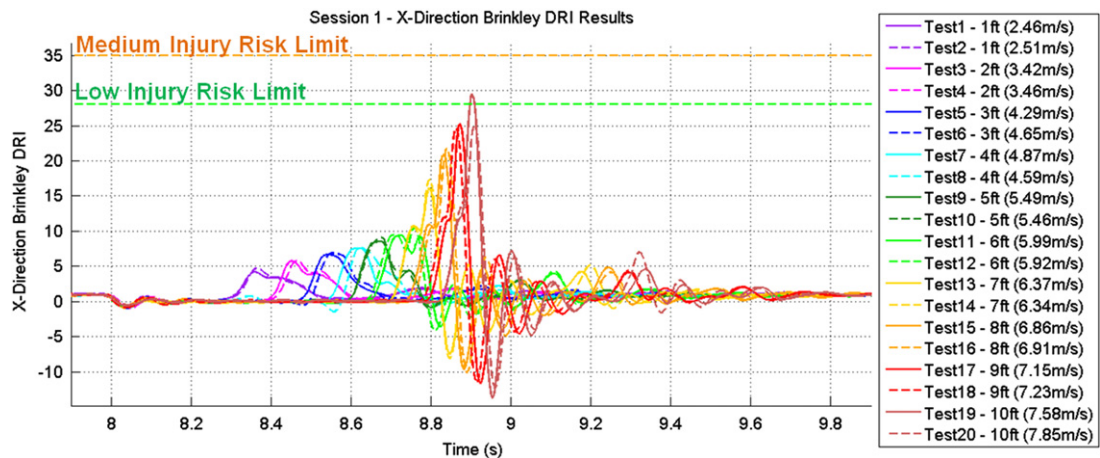


Fig. 15. Test session 1 X-direction Brinkley DRI results.

Here, it can be seen that at the 10 ft drop height, one of the drops remained within the low-injury risk limit while the other exceeded it. Interestingly, the drop test with the higher impact velocity of 7.85 m/s met the safety requirements, whereas the 7.58 m/s drop failed to meet them. Since the nominal impact velocity of Orion is 7.62 m/s (25 fps) [12], this suggests that at a 0° impact angle and under nominal impact velocities, the system is at the limit of its impact attenuation performance. Moreover, because the system was designed to prove concept feasibility, any improvement in performance resulting from more rigorous design and analysis, should produce a system which consistently meets all Brinkley criteria under these land-landing conditions. As a result, it can be stated that:

The airbag-based crew impact attenuation concept is feasible

In addition to this preliminary analysis, an investigation was conducted to determine why the as-built system had only just met the Brinkley low-injury risk criteria during the 0° impact case, when the predictions made during the

design process indicated that it should have easily met this requirement (see Table 3). In particular, this study focused on Test 19—the only 0° degree drop test to exceed the low injury-risk limits, and was accomplished by time synchronizing and over-plotting all obtained data to observe the interactions between the measured properties. This in turn allowed dynamic events of interest to be mapped to the resulting x-direction acceleration profile. The result of this is shown in Fig. 16.

Here, it can be seen that the side valves open shortly after the airbags begin to stroke. When the cumulative total area of the valves reaches its peak, the system reaches its first acceleration peak. This suggests that as the airbags stroke and the pressure relief valves open, the acceleration and corresponding pressure increases until the peak opening area is achieved. At this moment, the effect of the gas vented from the airbags causes the experienced acceleration to decrease. As this occurs, the airbag continues to stroke until either the system comes to rest or the stroke is depleted, causing a bottoming-out event to occur. For this particular case, the latter scenario was experienced, causing

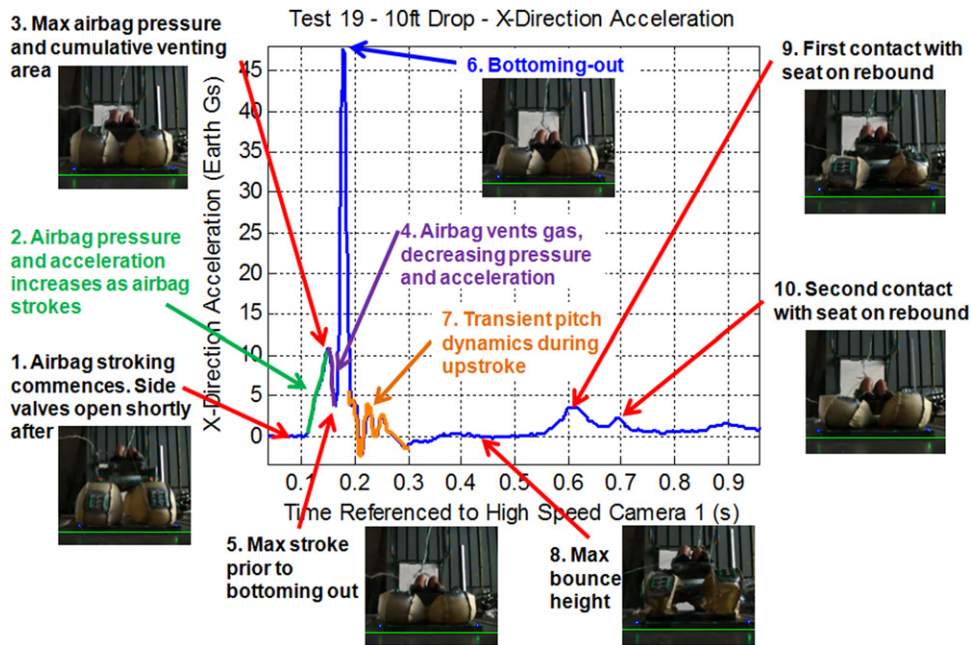


Fig. 16. Session 1 test 19 dynamically tagged X-direction acceleration response.

a subsequent sharp acceleration spike. Here, the correlation between this spike and a bottoming event was verified using high speed camera footage.

Following this bottoming-out event, the system was found to experience transient pitch dynamics as it bounced off the ground surface. After reaching its maximum bounce height, the system experienced a second impact with the ground, registering two miniature peaks in the acceleration response as various parts of the system came into contact with the ground surface.

Using this newly obtained insight, the entire Test Session 1 data set was revisited in an attempt to gain additional insight into the system performance. From this, it was found that the system dynamics is a superposition of the natural airbag dynamics, and the dynamics of bottoming-out. Specifically, this refers to the natural functions of airbag compression, pressure build-up, and venting characterized by the first peak observed in the acceleration response; and the bottoming-out dynamics characterized by the acceleration spike occurring shortly thereafter. This suggests that if this bottoming-out dynamics can be prevented, the overall system performance can be vastly improved due to the consequent reduction in peak acceleration and corresponding Brinkley Index. This can be seen in Fig. 17, where the peak acceleration for the 10 ft drop case would be 12.6 G's if bottoming-out were prevented. Interestingly, this potential peak acceleration is very close to the 11.8 G peak acceleration value predicted by the multi-airbag model for the 0° impact case. In regards to the corresponding injury-risk, this equates to a reduction in the peak Brinkley DRI value by a factor of at least 2, based on the stiffness and damping ratio values of the Brinkley model in the *x*-direction (see Table 2).

From a practical point of view, this motivates the need to explore the implementation of anti-bottoming airbags

within the system—an additional airbag whose purpose is to prevent direct contact between the payload mass and the impacting surface. Typically installed in a “bag within a bag” configuration, it is hypothesized that by adding anti-bottoming airbags, the influence of bottoming-out on the overall system dynamics will be largely mitigated. Fig. 18 shows one such example of this concept.

7.2. Test session 2 results (30° impact angle)

This section presents the analysis of the Test Session 2 results. Here, the same approach as that used in Section 7.1 was employed. Fig. 19 presents the injury-risk data obtained for all Session 2 drop tests, while Table A3 in the Appendix summarizes the entire dataset obtained.

Here, it can be seen that the system does not perform adequately during 30° impact angles, with the low-injury risk criteria being exceeded at drop heights of 5 ft, the medium injury-risk criteria being exceeded at drop heights of 6 ft, and the high injury-risk criteria being exceeded during the failed drop test at 7 ft. Considering the fact that all of these failed drops had impact velocities less than the nominal 7.62 m/s, this result definitively verifies the original NESC finding discussed in Section 5, stating that flatter angles are more favorable for land-landings.

As a consequence of this, a study was initiated to determine the reasons as to why the system performed so poorly at the 30° impact angle. Here, the same process as that used in the analysis of the Test Session 1 results was employed, whereby all data sources were time synchronized and over-plotted to investigate their interactions. In addition, a line detection scheme was implemented so that attitude information could be extracted from the high speed camera footage. For this particular study, the

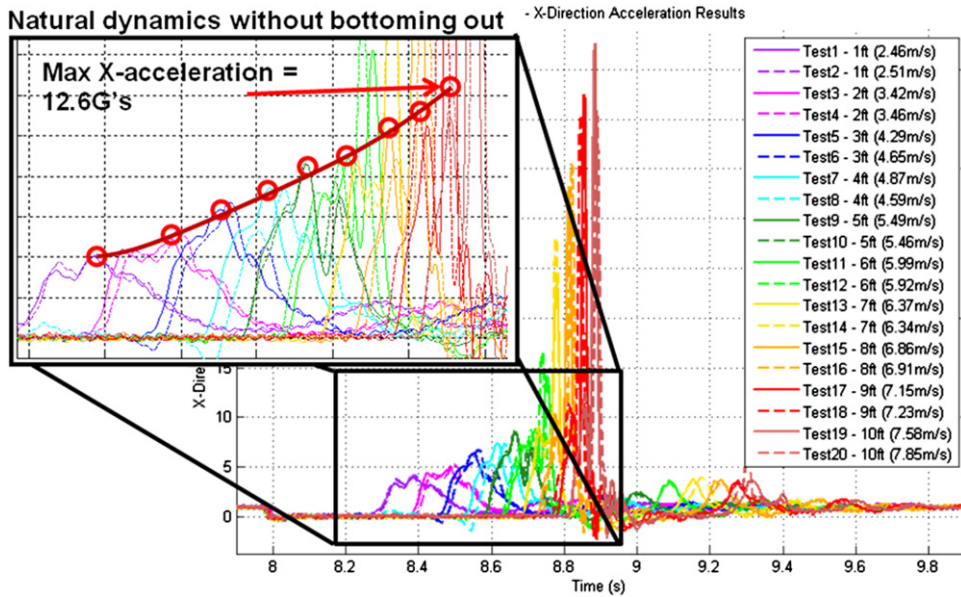


Fig. 17. Potential system dynamics without bottoming-out.

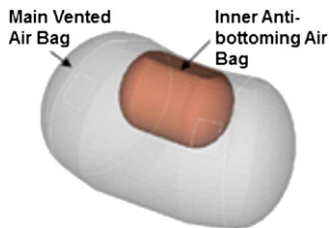


Fig. 18. Anti-bottoming airbag concept [13].

7 ft drop was chosen as the baseline, as it was the worst performing test case. Fig. 20 summarizes the results of this analysis.

From Fig. 20, it can be seen that shortly after the first acceleration peak, the system experiences a bottoming out event, as observed in the Test Session 1 results. Here, the short period of decreasing acceleration between the first and second acceleration spikes indicates that there was significantly less stroke in the airbags prior to bottoming-out, when compared to the 0° impact case. Again, following this bottoming-out event, the system experiences the previously observed transient pitch dynamics during its rebound, after which it obtains a maximum pitch angle during the peak height of its bounce. This pitch angle, in turn, causes the system to experience a second impact at an inclined angle.

Comparing this dynamically tagged response to the high speed camera footage, it was further noticed that all peak acceleration events occurred as a result of the head-ward end (refer to Fig. 14(a)) of the seat pivoting about the foot-ward airbags. This is a result of the differential stroking of the foot-ward and head-ward airbags, causing the head-ward end of the seat to pivot towards the ground about the feet as it continued to fall. As the seat pivoted about the foot-ward airbags, it sheared forward

relative to the simulated floor, removing a significant amount of stroke from the head-ward airbags. This hence explains the short decrease in acceleration between the first and second acceleration peaks observed in Fig. 20. Furthermore, by the time the head-ward airbags began to stroke, most of the air in the foot-ward airbags had already been depleted, causing this foot-ward end to continue to act as a pivot point for consequent rebounds of the system (see Fig. 21).

The presence of this shearing effect suggests that the three row configuration shown in the pink ellipse and found on the Pareto front in Fig. 12 may have been preferable in the design of the airbag configuration. The inclusion of an additional row of airbags between the existing airbags could potentially compensate for the lost stroke in the head-ward airbags due to the forward shearing motion. In turn, this would increase the time over which the acceleration response decreases after the first peak, thereby reducing the magnitude of any subsequent bottoming-out event.

7.3. System level impacts of implementing the personal airbag system

Given the observations made in Sections 7.1 and 7.2, three areas of the Orion system architecture have been identified as requiring some level of modification, in order for a personal airbag system to facilitate safe and reliable land-landings. These are:

- A change in the hang angle of the spacecraft underneath its parachutes from 30° to 0° . This arises from the finding that flatter impact angles result in lower injury-risk exposures to the crew during land-landings. From Tables A2 and A3 in the Appendix, it can be seen that as the drop height increased, the percentage increase in the Brinkley DRI of a 30° impact

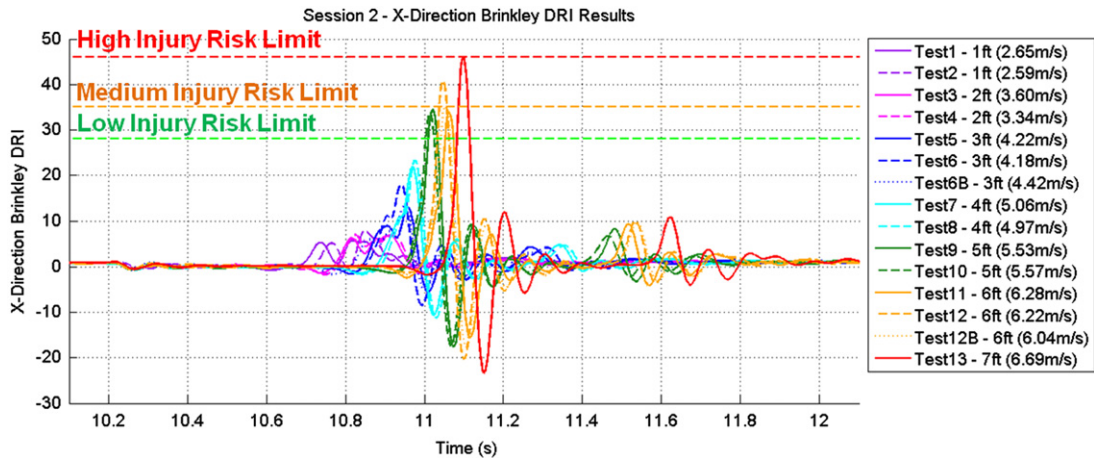


Fig. 19. Test Session 2 X-direction Brinkley DRI results.

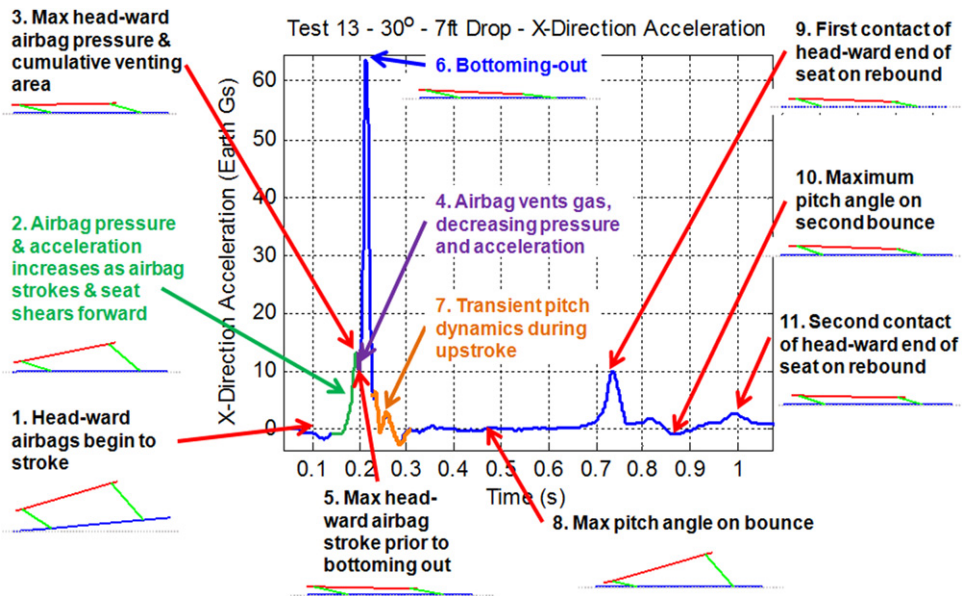


Fig. 20. Session 2 test 13—dynamically tagged X-direction acceleration response with resimulated dynamics shown underneath each tag (red line=seat, blue line=simulated spacecraft floor, green line=vector connecting airbag attachment points on system). (For interpretation of the references to color in this figure legend, the reader is referred to the web version of this article.)

as compared to a 0° impact increased substantially. At a 1 ft drop height, the 30° impact DRI was on average about 50% greater than the DRI at a 0° impact. Contrastingly, at a 7 ft drop height, the DRI of a 30° impact was on average 174% greater than the DRI of a 0° impact. Although no injury-risk data was obtained for impact angles between 0° and 30°, this large difference in DRI values indicates that the injury risk exposure to the crew may be sensitive to the spacecraft hang angle. This may become critical during landings with high horizontal wind speeds, which can blow the spacecraft away from its nominal hang angle. Moreover, such horizontal winds would contribute to the relative shearing effect between the crew seats and the spacecraft floor, as observed in Fig. 21(c). In this regard, it appears that some means of impact attenuation

implemented specifically for the lateral (*y*- and *z*-) directions is required. This may be in the form of airbags, dampening struts, or some other means.

- The implementation of some means of mitigating the risk of collision between adjacent seats during landing. This newly derived risk arises from the fact that using a personal airbag system for each crew member introduces the effects of differential stroking between each individual. During landings with high horizontal velocities, this effect can result in collisions between crew members seated next to each other. Although the forces imparted by such collisions will likely be lower than those experienced during the actual landing impact, this new source of injury risk is cause for concern. A possible means of mitigating this effect is to remove the lateral

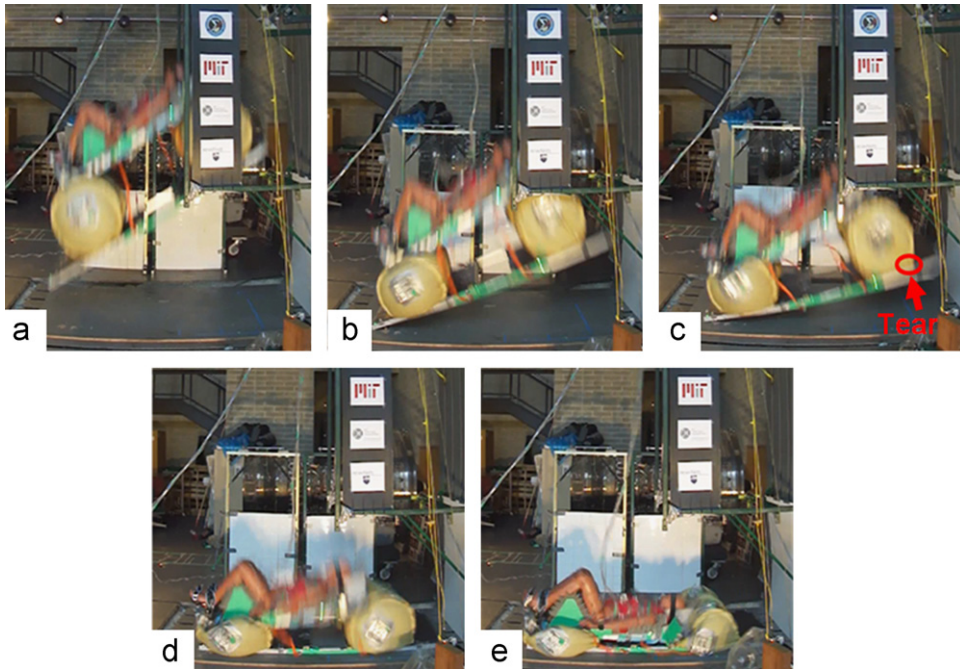


Fig. 21. Frame by frame breakdown of the 7 ft, 30° impact angle drop. (a) System in free-fall. (b) Differential stroking between foot-ward and head-ward airbags as the system makes first contact with the ground surface. (c) Forward shearing of the seat system relative to the simulated spacecraft floor. Also shown here is the location of the tear experienced during this drop. (d) Start of the head-ward airbag stroke. Note that a significant amount of stroke from these airbags has been removed due to the forward shearing of the seat system. Additionally, most of the air in the foot-ward airbags has been depleted by this point, causing them to act as a pivot point. (e) The system at rest after multiple impacts of the head-ward end of the seat with the ground surface.

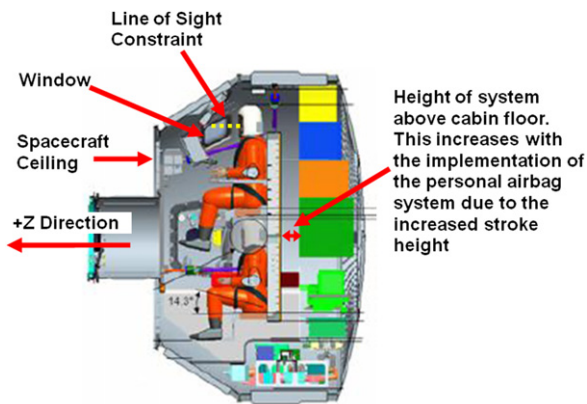


Fig. 22. Line of Sight constraints within the existing Orion spacecraft cabin (Adapted from Fig. 13 of Ref. [3]).

degrees of freedom between adjacent seats by some form of cross strapping. Such a concept is depicted in the ideation process shown in Fig. 2. By removing these degrees of freedom, the seats essentially connect to each other to form a pallet, similar to the supporting pallet currently baselined for Orion (see Fig. 1).

- A means of enabling the crew to see outside of the spacecraft during proximity operations and inspection and dynamic phases of a mission. This arises from the fact that the baselined impact attenuation system for Orion was designed such that

the crew had a direct line of sight through the vehicle's windows at all times (see Fig. 22). Because the height of the personal airbag system is greater than that of the baselined system, the line of sight of a crew member seated in the alternative system would not be aligned with the fixed position of the cabin windows. One option for resolving this would be to implement a video feed to the pilot's display, thus negating the need for a direct line of sight. This appears to be a simple solution with minimal impact on the rest of the system architecture.

Interestingly, the above modifications appear to impose a relatively small mass penalty to the current design. To a first order approximation, changing the spacecraft hang angle can be viewed as rearranging the pivot point of existing parachute lines, cross strapping the crew seats to prevent relative motion in the lateral directions can be achieved with light-weight tethers or stiffening members, and implementing a video-based line of sight involves installing cameras (which can be very low in mass) and wiring to connect these cameras to existing displays. Moreover, any additional impact attenuation mechanisms installed to accommodate the lateral directions will have masses less than or equal to that of the y - and z -direction struts currently proposed for Orion. This is because the existing struts can act as the default design option if a lighter mass alternative is not available. Even if these same struts were incorporated, the personal airbag system would result in an overall lighter system, due to the replacement of the x -direction

struts and the rigid pallet with a series of lower mass airbags.

No other system level impacts have been identified as a result of the implementation of personal airbag system within the Orion cabin. This is because the system uses the existing cabin atmosphere, can be inflated well before reentry using a simple electric or hand pump, and can be reconfigured according to a given mission phase. These attributes signify a self-contained solution that is capable of facilitating nominal land-landings with a mass penalty 24% lower than that of the baselined Orion impact attenuation system (see Table A1).

8. Conclusion

A full scale personal airbag system was designed, developed and subjected to an extensive drop test campaign to investigate its impact attenuation performance. Through this effort, this concept has been proven to be feasible. This feasibility is further verified by the fact that all drop tests were performed on land, with the only means of impact attenuation being the airbag system. This contrasts significantly to the more benign nominal Orion landing scenario of water landings attenuated by both crushable structures and strut-based mechanical damping. Moreover, the fact that the final developed system met these objectives while being 24% lighter than the baseline Orion system provides further support for airbag-based crew impact attenuation, especially given the fact that no mass optimization was actively performed on the design of the seat structure used to support the occupant.

Additionally, this study has yielded two key insights into the performance of the personal airbag system. The first of which being that the dynamic response of the system during impact is a superposition of the natural airbag dynamics and the dynamics of bottoming-out. By mitigating the effects of bottoming-out, it was found that the resulting peak Brinkley response under nominal landing conditions could be more than halved. This in turn motivates the need to explore the implementation of anti-bottoming airbags into the system.

The second important insight gained is related to why inclined impacts are so much more injurious than impacts

at flatter angles. Here, it was found that this was due to a combination of differential stroking between the front and rear airbags, and a consequent forward shearing motion between the seat and the spacecraft floor. The resultant effect of this was the removal of a significant amount of stroke from the head-ward airbags, and the pivoting of the system about the foot-ward airbags causing further impacts at the head-ward end of the system. Moreover, the presence of the observed shearing effect motivates the need to revisit the design of the airbag configuration, where the inclusion of an additional row of airbags may potentially offset the adverse effects of this shearing motion.

With regard to the implementation of personal airbag system aboard Orion and other future spacecraft, these findings have both upstream and downstream implications on the spacecraft design. These include the need for a flatter impact angle, and hence a near 0° hang angle of the spacecraft underneath its parachutes; as well as the configuration of the crew cabin, where variables such as the cabin geometry, crew relative positioning constraints relative to the spacecraft controls and viewing ports, and stowage constraints, will drive the design of the airbag-based system. A preliminary analysis of these system level impacts has concluded that the mass penalty of the necessary modifications is offset by the mass savings introduced by the personal airbag system. Therefore, this study has proven that this concept is capable of performing the fundamental function of protecting astronauts from the impact loads incurred during land-landings, with a lower mass penalty than that of current systems and a minimal impact on the existing system architecture. This finding thus warrants the inclusion of this concept in the Earth landing system tradespace of the next generation of piloted spacecraft.

Acknowledgments

Financial support for this research was provided by the NASA Engineering Safety Center (NESC) and the Constellation University Institutes Program (CUIP) under prime award number NCC3989 and subaward Z634013. The authors would like to thank Joe Pellicciotti, Tim Brady,

Table A1

Mass comparison between the baseline Orion crew impact attenuation system and the personal airbag system.

Orion crew impact attenuation system		Generation 2 personal airbag system	
Component	Mass	Component	Mass
Crew Seats		Crew Seats (6 total)	27.7 kg (61 lb) each
Operators 1 and 2	31.3 kg (69 lb) each		
Operators 3–6	27.4 kg (60.5 lb) each		
System support structure		System support structure	
Pallet Struts (9 total: 4-X, 3-Y, 2-Z)	10.9 kg (24 lb) each (average)	Integrated airbag (4 per crew member)	4.0 kg (8.8 lb) each
Miscellaneous components supported by system	100 kg (221 lb)	Inflation system (estimated mass)	11.3 kg (25 lb)
		Miscellaneous components supported by system	100 kg (221 lb)
Total mass	493.5 kg (1088 lb)	Total mass	373 kg (823 lb)

Table A2

Summary of personal airbag system drop test session 1 (0° impact angle) results.

Test no.	Drop height (ft)	Impact velocity (m/s)	Max X-acceleration (G's)	Max Brinkley DRx
1	1	2.46	4.004	4.23
2	1	2.51	4.128	4.71
3	2	3.42	4.923	5.77
4	2	3.46	5.302	5.77
5	3	4.29	6.356	6.73
6	3	4.65	6.689	6.90
7	4	4.87	7.427	7.59
8	4	4.59	7.384	7.70
9	5	5.49	8.575	8.57
10	5	5.46	8.643	9.12
11	6	N/A	14.208	9.42
12	6	5.92	16.562	10.51
13	7	6.37	23.444	16.10
14	7	6.34	28.068	17.38
15	8	6.86	33.178	20.95
16	8	N/A	35.472	21.73
17	9	7.15	42.474	25.28
18	9	7.23	40.451	24.70
19	10	7.58	47.544	29.46
20	10	7.85	40.298	25.09

NB. "N/A" implies that the high speed camera footage captured did not provide enough information to extract the stated variable.

Table A3

Summary of personal airbag system drop test session 2 (30° impact angle) results.

Test no.	Drop height (ft)	Impact velocity (m/s)	Max X-acceleration (G's)	Max Brinkley DRx
1	1	2.65	6.714	5.79
2	1	2.59	7.277	7.75
3	2	3.6	8.089	6.84
4	2	3.34	7.986	6.97
5	3	4.22	17.428	12.91
6	3	4.18	27.897	18.05
6B	3	4.42	17.476	13.27
7	4	5.06	32.353	21.83
8	4	4.97	36.103	23.22
9	5	5.53	47.274	34.45
10	5	5.57	46.522	33.65
11	6	6.28	53.321	33.95
12	6	6.22	53.359	40.79
12B	6	6.04	48.074	35.25
13	7	6.69	63.754	45.91

Charlie Camarda, Chuck Lawrence, Cory Powell and Ed Fasanella of the NESC for their technical support of this work; Lisa Jones and her team at NASA LaRC for their assistance with the loan of a Hybrid II crash test dummy; and the anonymous reviewers who provided valuable feedback on this article. Many thanks also go to Todd Billings, Dave Robertson, and Dick Perdichizzi of the MIT Department of Aeronautics and Astronautics for their invaluable contribution to the manufacturing and integration of the hardware developed throughout this project. Finally, this

project could not have been completed without the efforts of the numerous undergraduate students involved, from both the Massachusetts Institute of Technology and the Pennsylvania State University: Peter Cheung, Alban Cobi, Adrian Dobson, Josh Gafford, Daniel Goodman, Ricardo Robles Jr., Jackson Siu, Jared Trotter, and Jack Weinstein.

Appendix A

Table A1 presented is a mass comparison between the baseline Orion Crew Impact Attenuation System, and the personal airbag system. Here, the mass values for the Orion system were provided by the project sponsor. Tables A2 and A3 presented are a summary of all successfully performed drop tests with the personal airbag system.

Appendix B. Supplementary materials

Supplementary data associated with this article can be found in the online version at <http://dx.doi.org/10.1016/j.actaastro.2012.06.022>.

References

- [1] C.J. Johnson, R.A. Hixson, Orion vehicle descent, landing, and recovery system level trades, AIAA J. (2008) 7745.
- [2] J.D. Baker, D.J. Eisenman, D.E. Yucknovicz, Evaluation of Land versus Water Landings for Crew Exploration Vehicle, NASA Document RP-07-29.
- [3] C.J. Camarda, S. Bilen, O.L. de Weck, J. Yen, J. Matson, Innovative conceptual engineering design—a template to teach innovative problem solving of complex multidisciplinary design problems, AC 2010-1733, 2010 ASEE Annual Conference and Exposition, Louisville, KY, June 20–23, 2010.
- [4] C.E.J. Davis, N.P. Jahn, Qualification test of Apollo crew couch x-x axis foot cyclic impact strut assembly (V36-571711-121), North American Rockwell Corporation, NA-68-474, Los Angeles, CA, January 1969.
- [5] O.L. de Weck, Personal airbag system—NASA NESC research project overview, Presentation to NESC Orion Alternative Seat Attenuation Systems Team, March 17, 2009.
- [6] S. Do, O.L. de Weck, R. Robles Jr., J. Pellicciotti, T. Brady, An airbag-based crew impact attenuation system concept for the Orion cev—first generation system development, AIAA J. (2009) 6438.
- [7] B.W. Boehm, A spiral model of software development and enhancement, Comput. J. (1988) 61–72.
- [8] Do, S., An airbag-based crew impact attenuation system for the Orion crew exploration vehicle, S.M. Dissertation, Department of Aeronautics and Astronautics, Massachusetts Institute of Technology, Cambridge, MA, 2011.
- [9] NASA Constellation Program Human-Systems Integration Requirements, CxP 70024, Released 15 December, 2006.
- [10] C. Lawrence, E.L. Fasanella, A. Tabiei, J.W. Brinkley, D.M. Shemwell, The use of a vehicle acceleration exposure limit model and a finite element crash test dummy model to evaluate the risk of injuries during Orion crew module landings, NASA TM-2008-215198.
- [11] J.K. Cole, D.E. Wayne, BAG: a code for predicting the performance of a gas bag impact attenuation system for the PATHFINDER lander, SAND93-2133, November 1993.
- [12] C. Lawrence, K.S. Carney, J. Littell, Astronaut risk levels during crew module (CM) land landing, NASA GRC, NASA-TM-2007-214669, Cleveland, OH.
- [13] R.B. Timmers, R.C. Hardy, C.E. Willey, J.V. Welch, Modeling and simulation of the second-generation Orion crew module air bag landing system, AIAA J. (2009) 6593.



Sydney Do received a Bachelor of Engineering degree in Aerospace Engineering in 2008 from the University of Sydney, Australia, and a Master of Science in Aeronautics and Astronautics in 2011 from the Massachusetts Institute of Technology. He is currently a doctoral candidate in the Department of Aeronautics and Astronautics at the Massachusetts Institute of Technology. His research interests include Mars surface system architectures, and the sustainability of complex engineering systems.



Olivier de Weck is an Associate Professor of Aeronautics and Astronautics and Engineering Systems at the Massachusetts Institute of Technology (MIT). He holds degrees in industrial engineering from ETH Zurich (1993) in Switzerland and aerospace systems engineering from MIT (1999, 2001). He directs the Strategic Engineering Research Group at MIT, and is the Co-Director of the Center for Complex Engineering Systems at MIT and KACST in Saudi Arabia. He currently serves as Associate Editor for the Journal of Spacecraft and Rockets and the Journal of Mechanical Design. His research focuses on designing for lifecycle properties of complex engineering systems.